

Numerical and Experimental Optimization of Thermoelectric Modules for Power Generation

Min Chen¹, Jianzhong Zhang²; Lei Peng²; Dechang Zhang²;
Lili Zhang²; Lasse Rosendahl¹; Thomas Condra¹

1- Institute of Energy Technology, Aalborg University, Pontoppidanstræde 101,
Aalborg, DK-9220, Denmark

2- Tianjin Institute of Power Sources, Tianjin, 300381, China

Contact author:mch@iet.aau.dk

Introduction: In the application of thermoelectric power technique, the term optimization in a broad sense involves the design of all components in the energy system, i.e., the thermal system, the electrical system, and the thermoelectric device itself. Since their behaviors are strongly coupled, the optimization task demands for accurate numerical models for each above mentioned sector, and that these thermal and electrical models need then be run together. So far such a versatile tool to perform all simulations and designs as a whole has not been available.

This paper is to study the optimal design of thermoelectric generator modules based on a combined finite difference and Newton-Raphson numerical scheme [1]. The thermoelectric model presented therein is implemented in the circuit simulator SPICE, hence especially helpful for electrical system design. However, the model can also be used in the optimization of thermoelectric modules, provided that the boundary conditions of the thermal system and an equivalent resistor of the load circuit are extracted.

Method: The thermoelectric model in [1] accounts for all temperature dependent characteristics of the p- and n-type semiconductor material properties. Other input parameters of the numerical model include device geometry, hot and cold sources temperature, load resistance, and parameters such as waterproof rubber layer conductance and thermal and electrical contact resistances, leading to non-ideal effects.

At this stage the thermoelectric module TEC1-12706 (with 127 pairs of thermocouples) made by Tianjin Institute of Power Sources, China, is studied. All the input parameters for the module, including the detailed temperature data of the n- and p-type bismuth telluride materials, are collected to predict the generator performance as the model output.

A module test rig is developed to experimentally verify the model output, where an electrical heater is used as the hot source and a closed water cycle system is used as the cold source for the module. Two TEC1-12706 modules with the most alike characteristics are selected from other eight modules to be installed in the symmetric structure of the rig [1].



Fig 1. Test rig picture.

Hot and cold source: In the development of test rig for thermoelectric devices, electrical heaters made by heating wire embedded in machinable ceramic blocks have been applied as the hot source [2]. However, the formation of trenches on the ceramic block surface involves difficult machining job and is very costly due to the hardness of the material. In addition, the

thickness of the ceramic heater is in a scale of millimeter, making the control of the surface heat loss more difficult.

A thin foil electrical heater, customized with polyester insulation to fit the module cross-section size, is used as the hot source in this work. Its two lead wires are connected with outputs of an AC power supply, of which the effective value of the power output is taken to determine the input energy flow to the module. The resistance of the heater is designed to be 50.2Ω at room temperature. The value can be designed to be as low as several ohms by changing the heating element pattern to facilitate the application of a single DC power supply.

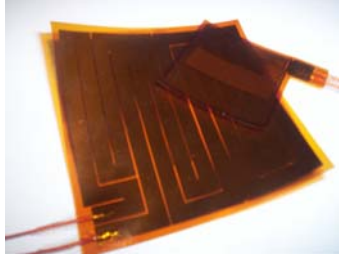


Fig 2. The customized polyester electrical heaters for thermoelectric modules.



Fig 3. The controllable coolant circulator HX-1050.

In the specification of the heater, the upper limit temperature is 150°C , for which the power density is recommended to be below $3\text{W}/\text{cm}^2$. In our practical experiment, we find that the heater temperature is only around 70°C - 80°C when the power density reaches $3\text{W}/\text{cm}^2$ because of the super heat sinking ability of the setup. The power applied is therefore further increased with a density higher than $3\text{W}/\text{cm}^2$ to yield the upper limit temperature. Higher temperature up to 200°C is possible for this test rig, since both the heating element and polyester are able to stand such a temperature. The glue used in the heater

might be melt, but because the heater is tightly clamped by the two modules, the heating effect as well as the temperature uniformity will not be influenced. Thus, although the polyester heater used herein is a low cost product, it can proffer an ideal heating effect at relatively high temperature range in this test rig, which is designed for thermoelectric devices.

In the cold side, the controllable circulator HX-1050 is used to drive the coolant, keeping a constant cold source temperature for the thermoelectric modules. The controlled constant temperature can be within the range from -10°C to 50°C .

Waterproof rubber layer: The thermal bypass effect of the waterproof rubber layer made from silicone adhesive sealant in the module TEC1-12706 is taken into account. To extract the parameter value of its equivalent resistor, the thermal conductivity of the rubber material is measured using a Quantum Design PPMS-9 at various temperature points. It is found out that the temperature dependent characteristic of the rubber conductivity is negligible. The thickness of the rubber layer is also measured, thus the effect of the waterproof rubber layer on the heat transfer is determined.



Fig 4. Rubber material sample and its conductivity measurement setup in PPMS.



Fig 5. Rubber layer in TEC1-12706 and its thickness measurement.

Contact resistances: Both the thermal and electrical interface effects are measured at room temperature through an indirect method. To obtain the electrical contact

resistance, firstly the total internal resistance of the module is measured at room temperature range (hot side 70 °C, cold side 30 °C) to be 2.55 Ω. Then the sum resistance of all n-type and p-type legs is calculated in terms of the material resistivities of 50 μΩ and the leg dimension (1.4mm*1.4mm*1.6mm), which is 2.33 Ω. Their difference 0.22 Ω is used as the electrical contact resistance value.

Similarly the thermal contact resistance, occurring at interfaces of all contacts between the hot and cold temperature measuring points, is experimentally determined by the above mentioned test rig, in which the load is disconnected to enable a constant heat flow to measure the total thermal resistance of heat transfer. When the hot side is at 25 °C and the cold side 15 °C the total thermal resistance of a single couple in the module (254K/W) is obtained by the temperature difference and the measured heat flow. The summed thermal resistance of the two legs and the waterproof rubber layer in one pair (243K/W) is calculated in terms of the material conductivities of 20 W/mK, the aforementioned leg and layer dimension. Their difference 11K/W is used as the thermal interface resistance value.

Results: The influence of the top and bottom ceramic layers of TEC1-12706 is firstly investigated. Their thermal resistance is determined by the known layer thickness (0.63mm) and conductivity value of Al₂O₃ ceramic. When compared with the simulation results of ideal condition, it can be seen from Fig 6 (circle and line) that little deterioration is caused by the ceramic layers in this case.

Secondly, it is found that the non-ideal effects caused by the heat conduction in the rubber layer and the thermal and electrical interface resistances, are fairly obvious. The distance between the dot-dash line and the circle line in Fig 6 shows that how much power generation performance improvement can be brought by optimizing these manufacturing parameters in the context of specific heat sources.

Finally, it is also found that the radiation from the top to the bottom ceramic layer inside the module does not have a significant effect on the power generation performance in this case.

Discussion: The error between the measurement and the simulation (with non-ideal effects) is enlarged as the hot side temperature increases. The discrepancy attributes to the change of the thermal and electrical interface resistances with temperature, and of model parameters with those in the real tested module. However, another reason for the error is the limitations of the rig. In the current rig, the coolant water in the closed cycle system flows through the cold side of two modules in a sequential order. Thus the cold side temperatures of two modules are not exactly the same. In most measurements there is a difference of several degrees, which make the heat flow from the heater not to be completely evenly distributed to the two modules. To improve the accuracy, the test rig can be refined by a parallel water circuit, where the coolant flows through the cold side of two modules in a simultaneous order.

Optimization: The effects of the geometry and dimension of the thermo-legs are the focus of the investigation, although the properties of the thermoelectric materials can be investigated by the same manner. From a practical viewpoint, the side length of the p-leg's square cross-section is changed from 1.2mm to 1.6mm, whilst the side length of the n-leg's cross-section is kept at 1.4mm. In Fig 7, the output current and power on the load increase with bigger p-leg cross-section, obviously due to the reduced generator internal resistance. We note that the actual temperature difference between the hot and cold junctions decreases with bigger p-leg cross-section, but this effect is not as big as that of the reduced internal resistance. Hence the output current and power are augmented in the range simulated.

For the conversion efficiency, however, p-leg cross-section has an optimum point

around 2mm^2 in the range of interest, where the efficiency is maximized (Fig 7 (c)). Since smaller leg cross-section means less consumption of thermoelectric materials, an

optimization at the device level on the leg cross-section area can be performed, provided that the efficiency is the main interest in the power specification.

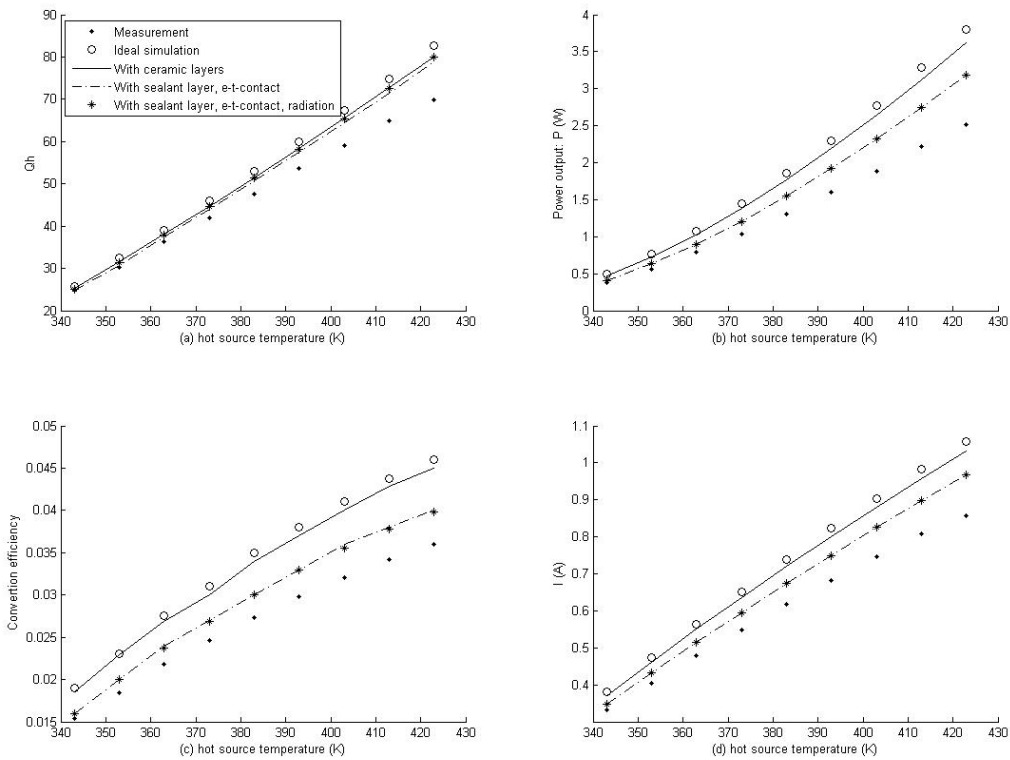


Fig 6. Comparison between various simulation and measured results for various temperature differences. The cold side temperature is fixed at 303K, and the load is 3.4Ω . (a) input heat flow, (b) power output, (c) efficiency, and (d) current.

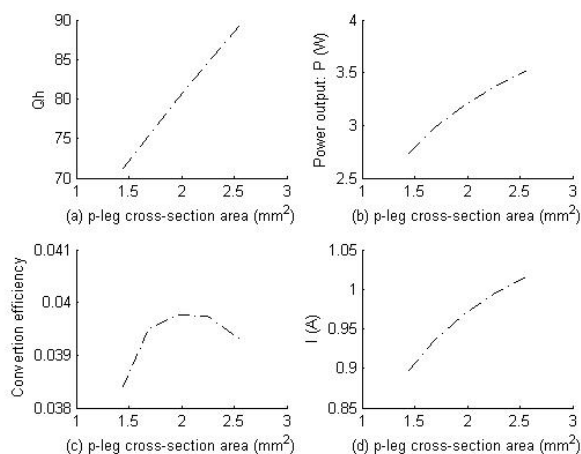


Fig 7. Simulation results for various p-leg cross-section areas. The hot and cold side temperatures are fixed at 423K and 303K, respectively. N-leg cross-section area is 1.96mm^2 and the load is 3.4Ω . (a) input heat flow, (b) power output, (c) efficiency, and (d) current.

Acknowledgment: A financial grant to the first author in connection with his research activities and studies in Tianjin is supported by The International Doctoral School of Technology and Science at Aalborg University.

- [1] M.Chen, L.A,Rosendahl, T.Condra, and J.K,Pedersen, Numerical Modeling of Thermoelectric Generators with Varing Material Properties in Circuit Simulator, (in preparation)
- [2] L Rauscher, S Fujimoto, H T Kaibe and S Sano, Efficiency determination and general characterization of thermoelectric generators using an absolute measurement of the heat flow, Meas. Sci. Technol. 16 (2005) 1054–1060